Journal of Engineering and Digital Technology (JEDT)
Vol.12 No.1 January - June 2024

Monitoring Blood Coagulation Behavior Using Quartz Crystal Microbalance with a Mason Equivalent Circuit Model

Sawit Na Songkhla[1] Wanida Laiwattanapaisal[2] Watcharee Boonlue[3*]

[1]*Faculty of Engineering, Chulalongkorn University, Bangkok, Thailand*
[2,3*]*Faculty of Allied Health Sciences, Chulalongkorn University, Bangkok, Thailand*

*Corresponding Author. E-mail address: watcharee.bo@chula.ac.th

Received: 6 February 2024; Revised: 26 February 2024; Accepted: 28 February 2024
Published online: 28 June 2024

Abstract

Blood clotting ability is a vital function of life forms, aiding survival when the body sustains cuts or wounds. Frequently, patients lacking this ability, or those on blood-thinning medications, can suffer from excessive bleeding, posing challenges for medical treatment. This is particularly relevant for dentists, as excessive bleeding may occur during tooth extractions or other dental procedures. Hence, there is a need for real-time blood coagulation detection. We propose using the quartz crystal microbalance (QCM) as a sensor. Its ability to detect mass loading and viscosity makes it feasible for coagulation testing in dental clinics. However, conventional equations like Sauerbrey's and Kanazawa's do not account for the dissipation factor, which plays a crucial role in determining liquid viscosity. We suggest using the Mason equivalent circuit model for interpreting blood viscosity and its clotting on the QCM surface. Observations show that film thickness increases with viscosity. Different samples exhibited varying viscosity changes, while the increase in film thickness was relatively comparable. This demonstrates the potential of the Mason equivalent Circuit model to differentiate results and estimate the underlying physical properties of blood coagulation.

***Keywords*:** Blood clotting, Mason equivalent circuit model, POCT, Quartz crystal microbalance

I. INTRODUCTION

Coagulation tests are essential in clinical diagnostics and treatment management. Their uses include diagnosing bleeding disorders, monitoring anticoagulant therapy, monitoring vitamin level, assessing vascular disease, and pre-surgical screening. In various coagulation assays, the time taken for viscosity changes is measured after adding an activator, using mechanical or optical methods. However, the complexity of preparing blood samples and activator agents is not conducive to on-site measurement or point of care testing (POCT). Since blood can be drawn directly from patients and coagulation can occur spontaneously from surface activation or certain pathways, the sensor required for this phenomenon can be simplified to a typical sensor.

Numerous biosensors have been developed for blood coagulation based on various principles, such as optical, surface plasmon resonance, magnetoelastic, or acoustic sensors. However, acoustic sensors like surface acoustic wave (SAW), film bulk acoustic resonator (FBAR), or quartz crystal microbalance (QCM) have the advantage of being able to measure viscosity changes during coagulation if the measurement circuit can extract loss or dissipation factors from the sensor [1].

The QCM sensor itself lacks affinity for specific molecules unless those molecules have an affinity for the metal electrode. Typically, QCM sensors require a sensitivity coating to achieve selectivity towards target molecules. These coatings can be polymers or biomaterials such as antibodies, enzymes, leptin, DNA, etc. Many of these coatings are viscous, rendering the conventional Sauerbrey equation for detecting rigid mass on QCM less accurate [2]. Coated QCMs have a wide range of applications as chemicals and biosensors. These applications include blood group identification [3], detection of cells, bacteria, and small molecules, gas sensing, and DNA analysis [4]–[6].

We propose using the QCM sensor to monitor coagulation due to its robustness and ability to detect viscosity. However, meaningful data interpretation is required. We applied the Mason equivalent circuit, initially proposed for use with viscous films in our previous investigation [7]. The Mason equivalent circuit Model is based on the coupling of acoustic impedance to electrical impedance. In this work, we further applied the model to data from human blood coagulation samples dropped directly onto a bare QCM electrode. Our focus is on explaining blood coagulation behavior in terms of film thickness and viscosity, as obtained from our model.

II. LITERATURE REVIEW

Measuring coagulation using whole blood samples offers a significant advantage over routine clinical tests such as prothrombin time (PT), activated partial thromboplastin time (aPTT), and platelet count. Whole blood coagulation assessment provides a comprehensive evaluation of hemostasis. It enables the measurement of fibrin formation and extends to clot retraction and fibrinolysis. This process facilitates the interaction of the plasma coagulation system with blood cells, including platelets.

Various biosensors have been developed as alternatives to traditional clinical tests. Munawar *et al.* utilized a QCM sensor to estimate PT, achieving significant reduction in plasma requirement compared to a standard mechanical coagulometer, with promising results (R^2 value of 0.99) [8]. Maji and team also introduced a sensor based on dielectric measurement to detect abnormalities in hemostasis, both non-cellular and cellular [9]. Cakmak *et al.* proposed a sophisticated microfluidic lab-on-chip (LoC) with nickel microcantilevers, actuated by a magnetic coil and measured using a laser doppler vibrometer (LDV), demonstrating reliable viscosity measurement with low coefficients of variation for PT

and aPTT [10]. Chen further advanced this field with the development of a very high frequency acoustic sensor, the FBAR, which showed excellent correlation and consistency in measuring prothrombin times when compared with commercial coagulometers [11].

Viscoelastic hemostasis assays, notably thrombo-elastography (TEG) and rotational thromboelastometry (ROTEM), stand out in the field for their ability to assess the viscoelastic properties of blood during clot formation and dissolution, offering a comprehensive perspective on the hemostatic process [12]. TEG utilizes a rotating cup with a torsion pin immersed in the blood sample to detect the torsional force from blood viscosity as coagulation progresses, while ROTEM follows a similar principle but with the pin itself rotating. These methods are advantageous for their ability to detect clot formation and dissolution, aiding in identifying clotting abnormalities. However, their use is limited due to the large volume of sample required and the potential for the rotation process to delay clot formation, which can distort the actual viscoelasticity of polymerization.

The QCM sensor operates on the piezoelectric principle, comprising an AT-cut quartz plate coupled with metal electrodes. When mass attaches to these electrodes, it leads to a decrease in the resonance frequency. Moreover, if the attached mass is non-rigid (or liquid), it causes additional damping or loss in the system. With its gravimetric effect and the ability to detect both mass and viscosity loading, combined with its relatively low cost, the QCM sensor becomes an attractive choice for detecting blood coagulation.

There is a wealth of publications on using the QCM sensor as a coagulation sensor, with studies focusing on measuring PT [8], [13], [14], aPTT [13], [15], [16], and thrombin time (TT) [17]. However, most of these studies did not aim to extract underlying parameters such as viscosity, density, or thickness of the coagulation aggregates. To gain a deeper understanding of the behavior during coagulation, it's important to consider a model that represents this process more comprehensively.

A precise model, such as the one proposed by Lucklum and Hauptmann in 2000, centers on the complex shear modulus $G_k = G' + jG''$, which defines both the elastic (G', elastic modulus) and viscous (G'', loss modulus) properties of blood [18]. This work involved simulating the Mason equivalent circuit under various conditions, including both lossy and lossless films in bulk liquid. The findings indicated that frequency changes were predominantly influenced by the film in contact with the QCM. Interestingly, the lossless film sometimes exhibited an unusual positive frequency change. While these studies may not have immediate real-world applications, they extensively explore the parameters of the Mason model, yielding significant insights from their simulations.

Bandey *et al.* analyzed the behavior of non-coagulating whole blood, erythrocyte sedimentation, and coagulation, discovering that non-coagulated whole blood acts as a viscous liquid primarily determined by plasma viscosity [19]. They noted that the penetration depth of liquid in plasma is approximately 300 nm, smaller than the size of RBCs, which must attach to the surface for QCM response observation. During sedimentation and coagulation, the attachment of elastic materials (RBC membranes and fibrin networks) interprets as an increase in G' and real (Zs) being greater than imag (Zs). Bandey had previously proposed a multi-layer analysis model [20], considering samples as consisting of two or more layers with distinct characteristics. Evans-Nguyen and Schoenfisch found that surface treatments (hydrophobic, hydrophilic, positively charged, negatively charged) significantly influence frequency response, particularly on hydrophilic surfaces [21]. They observed that fibrin filaments attach rigidly, behaving like mass loading as per the Sauerbrey equation [2].

Unfortunately, most literature simplifies the model to rigid mass [22], or like Muramatsu *et al.* [23], treats it as purely viscous semi-infinite material, lacking information on coagulation forming thickness and viscoelastic properties (G').

Our work also aims to utilize the Mason equivalent circuit model, simplifying it by reducing the parameters to a single-layer film. This approach is a preliminary step before delving into more complex parameters. We are attempting to determine the underlying viscosity and thickness of coagulated blood, achieving simplified yet reasonably accurate approximations.

III. RESEARCH METHODOLOGY

A. QCM Mason Equivalent Circuit

Typically, QCM as a sensor has a vastly used model near its resonant frequency called Butterworth–Van Dyke model (BVD) as shown in figure 1. We can analyze its equivalent impedance in terms of admittance, and it can be expressed as:

$$Y = \frac{1}{R_1 + j\omega L_1 + \frac{1}{j\omega C_1} + Z_{eL}} + j\omega C_0 \quad (1)$$

The BVD model integrates a series and parallel resonance circuit (motional branch), which includes L_1, C_1, and R_1. The electrodes on either side of the crystal plate add an extra parallel capacitance, C_0, resulting in the formation of a parallel circuit. Where Z_{eL} is the loading from the deposited viscous film. We usually simplify the model to film deposition which is useful for various conditions. Figure 2 shows a one-dimensional viscous model for the calculation. We consider the case of a viscous thin film, where ω is the angular frequency, m is the shear modulus, and v_{A1} is the shear wave velocity. The particle displacement u_1 and the shear stress T_5 are given by:

$$T_5 = \mu S_5 = \mu \frac{\partial u_1}{\partial x_3} = j\frac{\omega}{v_{A1}}\mu\left(-Ae^{-j\left(\frac{\omega}{v_{A1}}\right)x_3} + Be^{j\left(\frac{\omega}{v_{A1}}\right)x_3}\right) \quad (2)$$

Since A and B are constant, consider the stress free at film surface $(x_3 = t + h,\ T_{5=0})$. The ratio of A to B can be written as:

$$\frac{A}{B} = e^{j\left(\frac{2\omega}{v_{A1}}\right)(t+h)} \quad (3)$$

Substitute (3) into (2), The solution of the piezoelectric stress equation yields the acoustic impedance Z_L.

$$Z_L = -\frac{T_5}{j\omega u_1}\Big|_{x_3=t} = \frac{\mu}{v_{A1}}\frac{1-e^{j(2\omega/v_{A1})}}{1+e^{j(2\omega/v_{A1})}} = j\rho_L v_{A1}\, tan\left(\frac{\omega h}{v_{A1}}\right) \quad (4)$$

Where ρ_L represents the density of the film and h denotes its thickness, the shear wave in the viscous film was determined through a different method by replacing the shear wave with velocity in the stress equation, leading to the following result:

$$\rho_L \frac{\partial^2 u_1}{\partial t^2} = \frac{\partial T_5}{\partial x_3} \quad (5)$$

$$T_5 = j\omega\eta_L S_5 \quad (6)$$

And where η_L is the film viscosity. Applying equation (6) into (5) yield the wave velocity of the film

$$v_{A1} = \sqrt{\frac{j\omega\eta_L}{\rho_L}}. \quad (7)$$

Then, applying equation (7) to equation (4) we obtain

$$Z_L = j\sqrt{j\rho_L\eta_L\omega}\, tan\left(\sqrt{\frac{\rho_L}{j\omega\eta_L}}\right). \quad (8)$$

Electrical impedance Z_{eL} is expressed as

$$Z_{eL} = \frac{t^2 Z_L}{4e_{35}^2 S_A}, \quad (9)$$

where t is the quartz thickness, e_{35} is the piezoelectric constant, and S_A is the QCM electrode area.

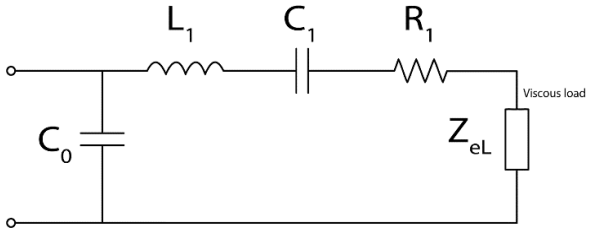

Figure 1: The equivalent circuit of the QCM, the Butterworth–Van Dyke model with viscous loading

The Vector Network Analyzer (VNWA) is used for extracting the QCM sensor's equivalent circuit components by measuring its conductance near the resonant frequency.

Impedance data across the frequency sweep range were analyzed and curve-fitted to determine R_1, L_1, and C_1, as depicted in Figure 1. This approach differs from the traditional motional admittance method, which only assesses the frequency at peak conductance. Our technique employs the entire data set for fitting to equation 1, aiming to minimize the mean square error for accurate circuit component determination. This method proves to be more reliable and less affected by noise compared to the standard motional admittance method.

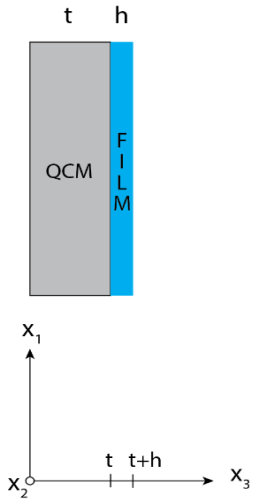

Figure 2: Model of the viscous film

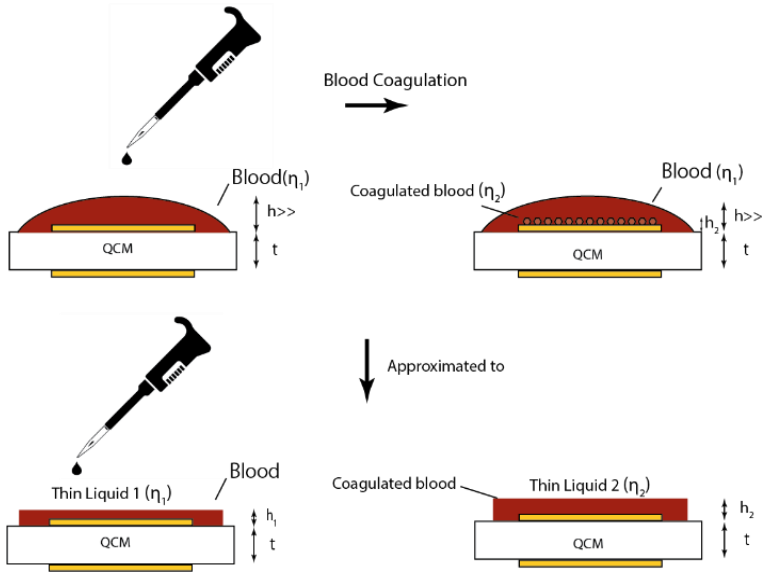

Figure 3: Model approximation blood coagulation from a single layer of viscous film with viscosity (η_1) and film thickness (h_1) into a film with different viscosity (η_2) and film thickness (h_2)

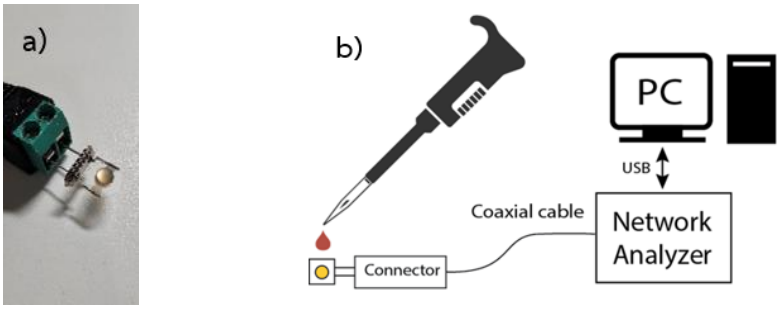

a) Image of QCM during experimentation b) Block diagram of QCM measurement system

Figure 4: Experimental setup for measurement for blood coagulation test

B. Blood Coagulation Response Approximation to Mason Equivalent Circuit

Figure 3 illustrates the approximation of the blood coagulation process as a single film layer, which changes in both thickness and viscosity. This representation differs from the actual bulk liquid of blood and the coagulation that occurs, potentially creating a film layer directly on the QCM surface. While this approximation may seem drastically inaccurate, it can be conceptualized that the bulk liquid is represented by a viscous film with a known thickness and viscosity. This simplification aids in interpreting the model and should adequately explain the experimental data according to the Mason circuit model of the single-layer film.

C. Measurement System

The QCM was specifically designed to resonate at 12.1 MHz. For measuring the S11 parameter of the QCM, a compact network analyzer (DG8AQ VNWA from SDR-Kits) connected through a coaxial cable was employed. The MATLAB software by MathWorks was used to facilitate these measurements. We scanned a frequency range from 12.115 MHz to 12.131 MHz, encompassing a 16 kHz span, each measured in 1.33 milliseconds. The selection of these parameters was an optimization from our earlier experiment [24]. The conductance curve, obtained from the S11 parameter through frequency scanning, utilized a 16 kHz range—twice the bandwidth of the curve for a Quartz Crystal Microbalance (QCM) in a 50% (w/w) aqueous glycerol solution. Measurements indicated that for this scanning range, the standard deviation was kept below 3 Hz, allowing quick sampling without much loss in precision. We collected 1000 data points within the scanning range, each at 1.33 milliseconds, amounting to a total of 1.33 seconds. Combined with the 16 kHz scanning range, this approach kept the scan time under 2 seconds, suitable for real-time applications. The configuration of our measurement system is illustrated in Figure 4.

IV. RESULTS AND DISCUSSION

A. aPTT Assay with Standard Serum, Coagulation Measurement Using QCM Sensor and Its Interpretation Using Mason Equivalent Circuit.

To perform the aPTT assay, we used platelet-poor plasma (PPP), reagents (including phospholipid and a contact activator specific to the aPTT), and calcium. We added 15 µL of the reagent to an equal volume of standard PPP (15 µL). Following this, we introduced 15 µL of 0.025 M calcium chloride ($CaCl_2$), initiating the clotting reaction. Subsequently, 15 µL of the resulting solution was carefully placed at the center of a QCM, ensuring full coverage of the electrode. This procedure was replicated five times. The raw data from the QCM experiments are presented in Figure 5. To clean the data of outliers, we employed the MATLAB function filloutliers, utilizing the median absolute deviation (MAD) method to identify outliers at three times its scale. Outliers were replaced using linear interpolation based on neighboring values, with the MAD window size set at 50 data points.

It's normal for the base frequency of each QCM to vary, due to manufacturing process tolerances. Our measurement system employs a vector network analyzer to extract the QCM's impedance. This method allows us to represent the motional impedance parts of the QCM through both resonant frequency and resistance, offering a more comprehensive analysis than merely reading the resonant frequency alone, as done in an oscillator circuit. Typically, we interpret the QCM's response through frequency changes. Around 100 seconds mark the point when the solution is deposited onto the QCM sensor, with the actual deposition time showing slight deviations due to the manual process. A significant drop in frequency and an increase in resistance were observed. Figure 6 displays shifts in both QCM frequency and resistance.

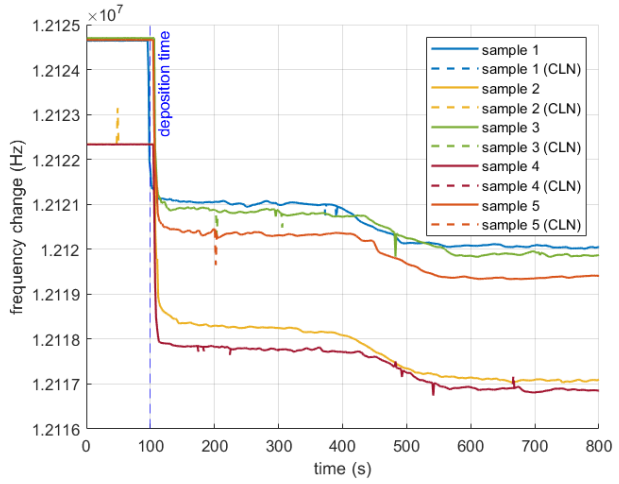

Figure 5: The raw frequency measurements from the QCM for five separate experiments of the aPTT assay using standard plasma

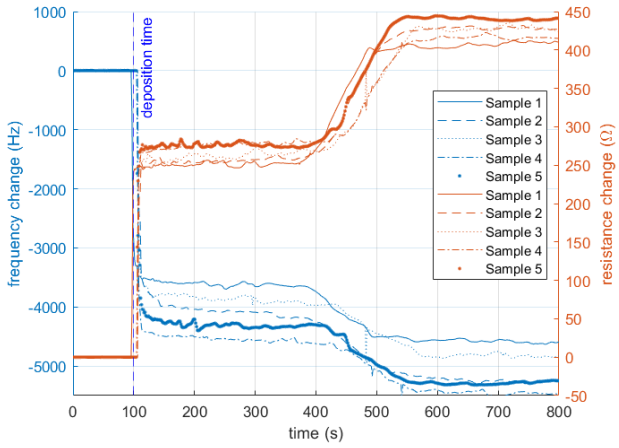

Figure 6: The changes in frequency and resistance measured by the QCM across five separate experiments of the aPTT assay using standard plasma

The coagulation process starts at around 400 seconds, as verified by visually inspecting the remaining solution. This was done by tilting it and then tapping and poking it with a pipette tip. Both the QCM results and visual inspection confirmed that coagulation was occurring simultaneously.

In the Mason equivalent circuit section, we identified three key variables related to coating film properties: film thickness (h), film viscosity (η_L), and film density (ρ_L), with an assumption of constant film density at 1 g/cm³. This assumption is integral to impedance derivation. We can convert resistance and frequency changes into impedance, which then allows for the calculation of film viscosity and thickness through specific equations. To integrate these test results into our models, we sampled data every 30 seconds after deposition for a total duration of 600 seconds. These data points were then plotted on a contour using a minimal numerical solver (fminsearch) in the applied equations. This approach enables us to estimate viscosity and film thickness, assuming a constant density of 1 g/cm^3.

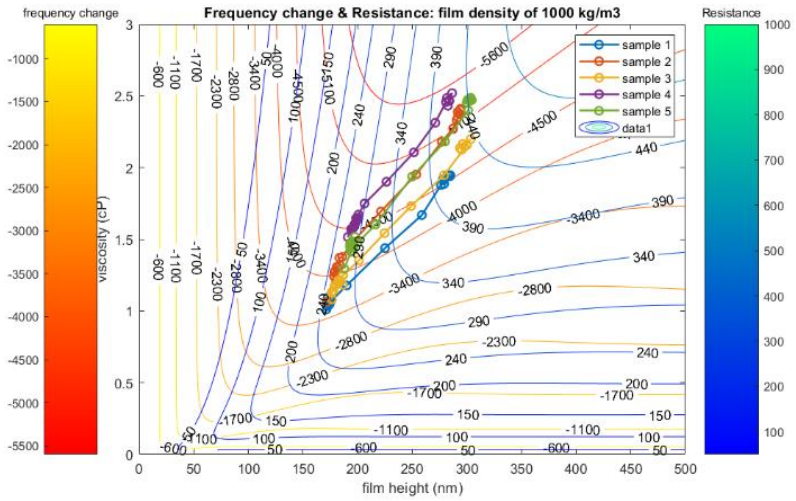

Figure 7: Combined contour plot of both resistance and frequency when across five separate experiments of the aPTT assay

Figure 7 converts the frequency and resistance shifts into a contour plot, mapping all data points collected up to 600 seconds after deposition onto a graph of viscosity and film thickness. The results indicate that as time progresses, the film's thickness increases from approximately 175 nm to 300 nm, and the viscosity changes from around 1 cP to 2.5 cP. These findings demonstrate the viability of our method for approximating changes in film thickness and plasma viscosity. The data from all five samples align closely within the contour plot, showcasing the method's repeatability. Furthermore, presenting the data in a plot of viscosity and film thickness facilitates easier interpretation of the results.

B. Whole Blood Coagulation Measurement Using QCM Sensor and Its Interpretation Using Mason Equivalent Circuit

We conducted an experiment focusing on blood deposition to study how blood coagulation affects the QCM. A micro pipette was used to precisely apply a 10 μL sample of whole blood directly onto the QCM electrode. These samples originated from two different human blood sources. Figure 8 illustrates the QCM's response over time, where notable changes in frequency and resistance are observed due to the deposition.

Immediately after the blood is deposited, a negative frequency shift occurs, indicative of a typical response to viscous loading. Over time, the resistance continues to increase, while the frequency shift gradually decreases. Eventually, the trend in frequency changes: it starts to increase, reversing its initial behavior, and eventually shifts to a positive value.

Interpreting this response solely using the Sauerbrey equation and Kanazawa theory proves insufficient. This is because we also have resistance data, and the specific condition of coagulating blood doesn't align with the mass loading conditions assumed in the Sauerbrey equation or the bulk liquid conditions of the Kanazawa equation. Furthermore, the coagulated blood may form a film-like layer at the electrode, suggesting that this scenario should be analyzed using the Mason equivalent circuit model.

We collected data every 30 seconds over a period of 600 seconds (10 minutes) post-deposition. These data points were then plotted on the contour using a minimum numerical solver (fminsearch) in the applied equations, enabling us to deduce viscosity and film thickness, while assuming a constant density.

The contour plot showing changes in frequency and resistance for a whole blood sample is depicted in Figure 9. The results obtained from the fminsearch are represented as circular points. However, mapped data points are available only for the first three instances following blood deposition (the first three circles from the left in Figure 8). This limitation stems from the equation solver's difficulty in identifying local minima with an acceptable mean square error (less than 10^{-3}). A detailed analysis of the contour plot highlights its constraints: it does not reflect the slight increase in frequency while resistance increases significantly, and as the film thickness grows, the contour lines for frequency and resistance shifts become almost parallel. The occurrence of frequency increase alongside resistance increase is not observed at greater film thicknesses. This observation implies that film thickness has a minimal effect on the changes in frequency and resistance, with viscosity playing a more significant role. Additionally, the plot does not account for positive frequency changes. Introducing complex viscosity into the Mason equivalent circuit model could explain these positive frequency shifts, but this complicates the equation's understanding and interpretation, warranting further study.

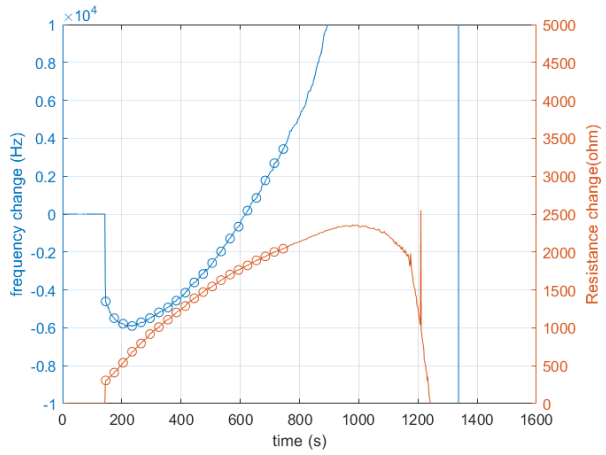

Figure 8: presents the QCM's response following the deposition of blood sample 1. The circled data points, used for mapping onto the Mason equivalent circuit plot, were sampled every 30 seconds

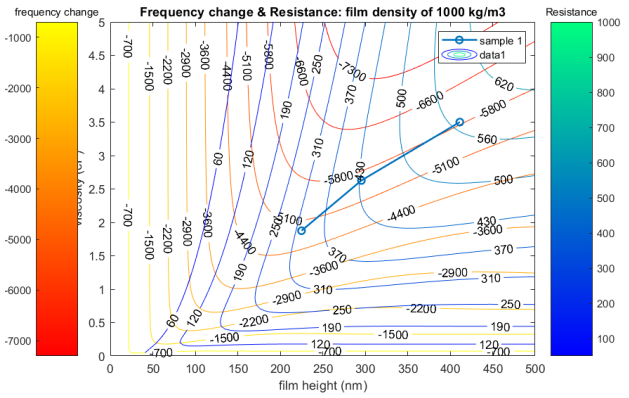

Figure 9: Combined contour plot of both resistance and frequency when blood is deposited onto QCM of blood sample 1

Despite these limitations, the interpretation remains useful for thin film layers, with the first three data points indicating that as coagulation progresses, both film thickness and viscosity increase. Yet, beyond a certain point, the frequency increases so much that it no longer fits the model meaningfully, suggesting a need to explore the concept of complex viscosity to rationalize the positive frequency shifts. Instances of increasing frequency upon deposition have been observed, such as in [18]. Their study, involving a Mason equivalent circuit model with a viscous film layer immersed in a bulk liquid, showed that under specific conditions (a 500 nm film thickness, with real and imaginary parts of the acoustic load Z_f at 2,721 and 17,697 Pa s m-1, respectively, immersed in a 10 cp viscosity liquid), a positive frequency shift is possible. Their simulation implies that in a high viscosity liquid with a low loss film, such positive frequency changes may occur.

V. CONCLUSION

In conclusion, the enhanced Mason equivalent circuit model, incorporating a viscous film boundary condition, has proven to be a highly effective tool for monitoring coagulation progress. Its strength is its ability to provide more definitive results than those obtained solely through cutoff values of frequency and resistance shifts. Our model offers a more intuitive and comparative analysis of coagulation by translating frequency and resistance data into viscosity and film thickness. This could make it comparable to other viscoelastic hemostasis assays.

Moreover, our model presents a faster approach to coagulation testing, eliminating the need for activators and potentially estimating coagulation times in under a minute without reagents. This significantly reduces both the operational costs and the time required for testing. This model can be a part of a point-of-care testing device for various applications, including preoperative screening before dental procedures and the result from the blood coagulation test can provide guidance on adjusting dietary habits to increase the intake of vitamin K from food sources.

It is also evident that focusing on thinner films, where the model remains effective, should be a priority. We have established its feasibility for film thicknesses up to approximately 400 nm. Initially, we overlooked the potential impact of bulk liquid on top of forming blood clots. Our current efforts are aimed at further validating the model with a larger sample size and incorporating a bulk liquid layer above the viscous layer to improve accuracy. Additionally, considering the

incorporation of the elastic modulus (G') to account for the viscoelastic properties of the film is an area for future improvement.

ACKNOWLEDGEMENT

This research was funded by grants for development of new faculty staff, Ratchadaphiseksomphot Endowment Fund.

REFERENCES

[1] A. Mujahid, A. Afzal, and F. L. Dickert, "An overview of high frequency acoustic sensors—QCMs, SAWs and FBARs—chemical and biochemical applications," *Sensors,* vol. 19, no. 20, p. 4395, Oct. 2019.

[2] G. Sauerbrey, "Verwendung von Schwingquarzen zur Wägung dünner Schichten und zur Mikrowägung," (in German), *Zeitschrift für Physik*, vol. 155, no. 2, pp. 206–222. Apr. 1959.

[3] A. Seifner, P. Lieberzeit, C. Jungbauer, and F. L. Dickert, "Synthetic receptors for selectively detecting erythrocyte ABO subgroups," *Analytica Chimica Acta*, vol. 651, no. 2, pp. 215–219, Oct. 2009.

[4] P. J. Jandas, K. Prabakaran, J. Luo, and M. G. D. Holaday, "Effective utilization of quartz crystal microbalance as a tool for biosensing applications," *Sensors and Actuators A: Physical*, vol. 331, Nov. 2021, Art. no. 113020.

[5] M. Jenik, A. Seifner, P. Lieberzeit, and F. L. Dickert, "Pollen-imprinted polyurethanes for QCM allergen sensors," *Anal. Bioanal. Chem.*, vol. 394, no. 2, pp. 523–528, Mar. 2009.

[6] M. Jenik *et al*., "Sensing picornaviruses using molecular imprinting techniques on a quartz crystal microbalance," *Anal. Chem.*, vol. 81, no. 13, pp. 5320–5326, Jul. 2009.

[7] S. N. Songkhla and T. Nakamoto, "Interpretation of quartz crystal microbalance behavior with viscous film using a mason equivalent circuit," *Chemosensors*, vol. 9, no. 1, p. 9, Jan. 2021.

[8] M. Hussain, "Prothrombin Time (PT) for human plasma on QCM-D platform: A better alternative to 'Gold Standard'," *Pharmaceutical Biosci. J.*, vol. 3, no. 6, pp. 1–8, Sep. 2015.

[9] D. Maji *et al.*, "Assessment of whole blood coagulation with a microfluidic dielectric sensor," *J. Thrombosis Haemostasis*, vol. 16, no. 10, pp. 2050–2056, Oct. 2018.

[10] O. Cakmak *et al.*, "A cartridge based sensor array platform for multiple coagulation measurements from plasma," *Lab Chip*, vol. 15, no. 1, pp. 113–120, Oct. 2015.

[11] D. Chen *et al.*, "Micro-electromechanical film bulk acoustic sensor for plasma and whole blood coagulation monitoring," *Biosensors Bioelectron.*, vol. 91, pp. 465–471, May 2017, doi: 10.1016/j.bios.2016.12.063.

[12] S. D. Sahli, J. Rössler, D. W. Tscholl, J. D. Studt, D. R. Spahn, and A. Kaserer, "Point-of-care diagnostics in coagulation management," *Sensors*, vol. 20, p. 4254, Jul. 2020.

[13] J. Yao *et al.*, "Blood coagulation testing smartphone platform using quartz crystal microbalance dissipation method," *Sensors*, vol. 18, no. 9, p. 3073, Sep. 2018.

[14] L. Müller *et al.*, "Investigation of prothrombin time in human whole-blood samples with a quartz crystal biosensor," *Anal. Chem.*, vol. 82, no. 2, pp. 658–663, Jan. 2010.

[15] M. Hussain, "Ultra-sensitive detection of heparin via aPTT using plastic antibodies on QCM-D platform," *RSC Adv.*, vol. 5, no. 68, pp. 54963–54970, Jun. 2015.

[16] Y. Yang *et al.*, "Stability enhanced, repeatability improved Parylene-C passivated on QCM sensor for aPTT measurement," *Biosensors Bioelectron.*, vol. 98, pp. 41–46, Dec. 2017, doi: 10.1016/j.bios.2017.06.021.

[17] W. Pan *et al.*, "Applicability of a sensitivity-enhanced quartz crystal microbalance in analyzing blood plasma viscosity and coagulation," *Sensors Mater.*, vol. 34, no. 4, pp. 1515–1525, Apr. 2022.

[18] R. Lucklum and P. Hauptmann, "The Δf–ΔR QCM technique: An approach to an advanced sensor signal interpretation," *Electrochim. Acta*, vol. 45, no. 22–23, pp. 3907–3916, Jul. 2000.

[19] H. L. Bandey, R. W. Cernosek, W. E. Lee III, and L. E. Ondrovic, "Blood rheological characterization using the thickness-shear mode resonator," *Biosensors Bioelectron.*, vol. 19, no. 12, pp. 1657–1665, Jul. 2004.

[20] H. L. Bandey, S. J. Martin, R. W. Cernosek, and A. R. Hillman, "Modeling the responses of thickness-shear mode resonators under various loading conditions," *Anal. Chem.*, vol. 71, no. 11, pp. 2205–2214, Jun. 1999.

[21] K. M. Evans-Nguyen and M. H. Schoenfisch, "Fibrin proliferation at model surfaces: Influence of surface properties," *Langmuir.*, vol. 21, no. 5, pp. 1691–1694, Mar. 2005.

[22] B. C. Heinze and J.-Y. Yoon, “Real-time monitoring of fibrinogen cross-linking on model biomaterial surfaces with quartz crystal microbalance,” *Open Biotechnol. J.*, vol. 2, no. 1, Nov. 2008.

[23] H. Muramatsu, J. Kim, and S. Chang, “Quartz-crystal sensors for biosensing and chemical analysis,” *Anal. Bioanal. Chem.*, vol. 372, no. 2, pp. 314–321, Jan. 2002.

[24] S. N. Songkhla and T. Nakamoto, “Signal processing of vector network analyzer measurement for quartz crystal microbalance with viscous damping,” *IEEE Sens. J.*, vol. 19, no. 22, pp. 10386–10392, Nov. 2019.